ECS Journal of Solid State Science and Technology, **1** (5) P222-P226 (2012)
2162-8769/2012/1(5)/P222/5/$28.00 © The Electrochemical Society

Low-Stress Highly-Conductive In-Situ Boron Doped $Ge_{0.7}Si_{0.3}$ Films by LPCVD

S. N. R. Kazmi,[z] A. Y. Kovalgin,[*] A. A. I. Aarnink, C. Salm,[z] and J. Schmitz

MESA+ Institute for Nanotechnology, University of Twente, 7500 AE Enschede, The Netherlands

This paper reports on low pressure chemical vapor deposited in-situ boron doped polycrystalline germanium-silicon layers with 70% germanium content. The effect of diborane partial pressure on the properties of the GeSi alloy is investigated. The obtained high boron concentration results in resistivity values less than 1 mΩ-cm. The layers deposited at low partial pressures of B_2H_6 exhibit very low stress down to –3 MPa. With increasing B_2H_6 partial pressure first the stress changes from tensile to compressive, followed by a phase transition from polycrystalline to amorphous. The highly doped, low stress poly-$Ge_{0.7}Si_{0.3}$ layers deposited at 430°C are further applied in high-*Q* microelectromechanical resonators envisaged for above-IC integration with CMOS.

[DOI: 10.1149/2.008205jss]

Manuscript submitted June 5, 2012; revised manuscript received August 13, 2012. Published August 29, 2012. This was Paper 2058 presented at the Montreal, QC, Canada, Meeting of the Society, May 1–6, 2011.

Germanium-silicon (GeSi) alloys are commonly applied in microelectronics; for instance, in heterojunction bipolar transistors;[1] and in gates[2,3] and source/drain regions of field-effect transistors.[4] Compared to pure silicon, processing of GeSi takes place at considerably lower temperature. Polycrystalline layers of GeSi can be deposited using Low Pressure Chemical Vapor Deposition (LPCVD) at temperatures below 450°C;[5] under similar conditions silicon deposits in amorphous form.

The relatively low temperature enables poly-GeSi applications in the backend (interconnect layers) of CMOS technology, where the temperature budget is limited (see e.g.[6,7]). The alloy has been proposed as sacrificial layer[8] for surface micromachining (making use of the ease of selective removal); and as a permanent (electrical-) mechanical layer, for example in MEMS resonators,[9] micromirrors and accelerometers.[10]

Application in surface-micromachined suspended structures further requires low residual stress in the film (and a low stress gradient). As stress is affected by a variety of parameters (such as Ge:Si ratio, deposition temperature and pressure, and impurity concentration), it can be regulated to some extent by a proper choice of process conditions. A low specific resistance is further required in several applications where GeSi acts as an electrode, such as accelerometers and resonators. Additional film requirements may concern stiffness, Young's modulus, density, surface roughness, thickness uniformity and reproducibility of the alloy composition.

LPCVD, chosen for its high throughput, uniformity and reproducibility,[11] naturally offers the possibility of in-situ doping by addition of an appropriate precursor gas, thus avoiding a high-temperature activation step for ion-implanted impurities. In-situ doped GeSi layers are usually deposited from GeH_4 and SiH_4 (or Si_2H_6) source gases with either B_2H_6/BCl_3 or PH_3 as dopant precursors for p-type or n-type doping, respectively.[12,13] B_2H_6 is chosen for the present work as it yields higher conductivity films at higher growth rate compared to PH_3 in-situ doped layers. Compared to BCl_3 it reacts (and decomposes) at a lower temperature,[14] allowing a reduced thermal budget.

In this work, we systematically investigate the impact of B_2H_6 partial pressure on the properties of LPCVD in-situ boron doped $Ge_{0.7}Si_{0.3}$ layers. We discuss the resistivity, residual stress, texture, surface roughness and chemical composition of the films. We also show a first application of the layers in a high-*Q* surface-micromachined resonator.

Experimental

In-situ boron doped poly GeSi layers were deposited on 100 mm single side polished ⟨100⟩ oriented Si wafers (381±15 µm, n-type/phosphorus doped, 1–10 Ω-cm) with 100 nm of thermally grown oxide. The wafers were directly loaded into a custom built hot-wall horizontal LPCVD reactor (Fig. 1) after cleaning in 99% HNO_3 for 5 minutes followed by DI water rinse and N_2 drying, maintained at a base pressure of 10^{-3} mbar. The pressure inside the furnace was raised to 10 mbar with 150 sccm of N_2 flow to uniformly heat up the wafers to 430°C for 30 minutes. A thin (few nm) amorphous silicon layer, acting as nucleation layer,[5] was deposited at 0.5 mbar and 430°C for 10 min with 88 sccm of SiH_4 flow.

The in-situ boron doped $Ge_{0.7}Si_{0.3}$ layers (targeting 500 nm) were then deposited from pure SiH_4 and pure GeH_4 gases with the addition of B_2H_6 diluted in Ar (B_2H_6/Ar). The total flow of (Ar+ B_2H_6/Ar) is constant at 100 sccm, with the B_2H_6 partial pressure varied to have a range of doping concentrations. All GeSi depositions are carried out at 430°C and 0.2 mbar total pressure with fixed SiH_4 and GeH_4 flow of 75 sccm and 37 sccm corresponding to partial pressures of $7.1 \cdot 10^{-2}$ mbar and $3.5 \cdot 10^{-2}$ mbar, respectively.

The gases were introduced from the front side of the LPCVD tube via mass flow controllers (MFCs). Each experiment involves nine process wafers surrounded by two dummy wafers in front and two at the back of the wafer boat. The gas depletion effect was minimized by maintaining high flow of reactive gases using roots blowers. The aim was to find deposition conditions below 450°C for a low-resistivity and low-stress GeSi alloy, for surface micromachining on top of foundry fabricated CMOS.

The thickness of deposited layers was measured using a Dektak 8.0 surface profilometer, averaged over five points, after a masked etch of GeSi in SF_6 and O_2 plasma. The residual stress in the deposited layers was determined, using Stoney's equation,[15] by measuring the wafer curvature before and after deposition (with the back side layer removed) in two orthogonal directions with Dektak 8.0. The resistivity was measured by the four probe measurement method, averaged over nine points across the wafer. Cross sectional high resolution secondary electron microscopy (HRSEM) images were taken to observe the morphology of in-situ doped GeSi layers. The surface roughness was measured with a Micromap interference microscope, with height resolution better than 1 nm, averaged over five different places on the wafer with an area of 125.4 µm by 94.08 µm.

X-ray diffraction (XRD) analysis was carried out with a Philips XRD model expert system II using the Cu K-α line of wavelength 1.54 Å to obtain information on the crystallinity of the deposited samples. The depth profile of Ge/Si contents was determined by X-ray Photoelectron Spectroscopy (XPS) using 5-keV argon sputtering.

Secondary Ion Mass Spectroscopy (SIMS) was performed to determine the boron concentration in the deposited layers. The SIMS analysis was performed using 3 keV O_2^+ primary ions bombardment with positive mode. The first ∼10 nm of the profiles are unreliable due to transient instrumental effects and also the profile region close to the oxide. The concentration determination within the oxide and in

---

[*] Electrochemical Society Active Member.

[z] E-mail: snrkazmi@gmail.com; C.Salm@utwente.nl

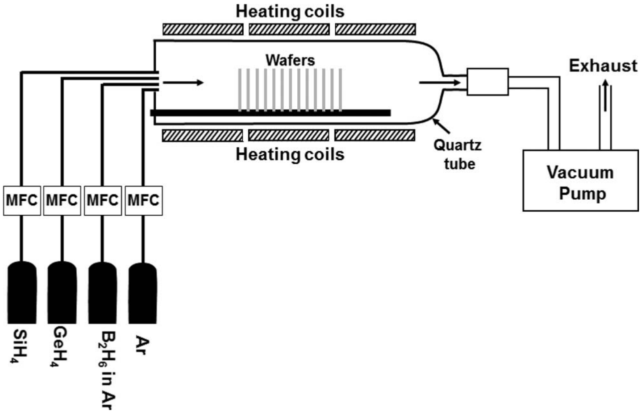

Figure 1. Schematic overview of the employed LPCVD system.

the neighboring regions is less accurate due to charging and matrix effects.

GeSi Material Properties

The deposition rate of in-situ boron doped $Ge_{0.7}Si_{0.3}$ increases from 3.2 nm/min to 6 nm/min with increasing B_2H_6 partial pressure from 0 mbar to $2.35 \cdot 10^{-3}$ mbar. This increase is in line with earlier reports and is attributed to the boron atoms acting as adsorption sites for both silicon and germanium atoms (see e.g.[11]). At diborane partial pressures beyond $2.35 \cdot 10^{-3}$ mbar a slight decrease of deposition rate is observed, which might be due to gas phase reactions. The variation in cross wafer and cross load thickness uniformity is 3.4% and 9.5% at most, respectively, for all the deposited layers.

The dependence of film resistivity on B_2H_6 partial pressure is plotted in Fig. 2. Initially the resistivity drops steeply, accompanied with a gradual increase in the boron concentration up to $1.2 \cdot 10^{21}$ cm^{-3} at $1.9 \cdot 10^{-4}$ mbar partial pressure, as found by SIMS. The resistivity then starts to increase with a further increase of the B_2H_6 partial pressure, eventually reaching 600 mΩ-cm, even higher than the resistivity of the undoped (or rather, not-intentionally-doped) poly-$Ge_{0.7}Si_{0.3}$ layer. This observed increase in resistivity is associated with a gradual transition from polycrystalline to amorphous phase, as treated later in this article. In these experiments, the worst case uniformity in resistivity along the waferboat and even on a single wafer can be observed for the diborane partial pressure of $2.35 \cdot 10^{-3}$ mbar. This leads to the cross wafer and cross load variation in resistivity of up to 14.7% and 21%, respectively.

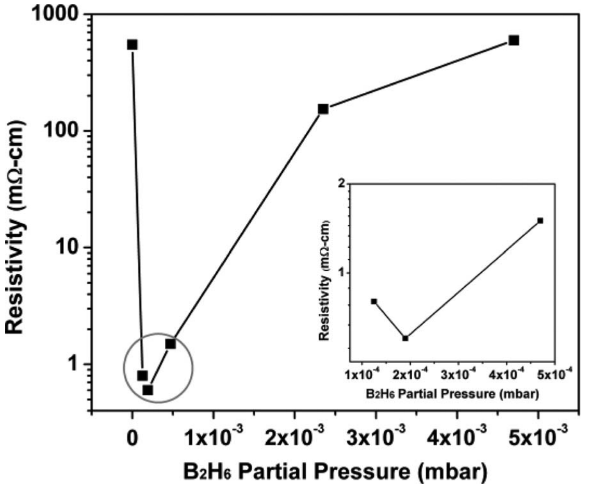

Figure 2. Resistivity vs. B_2H_6 partial pressure for ∼500 nm $Ge_{0.7}Si_{0.3}$ films deposited at 430°C and 0.2 mbar on thermally grown oxide.

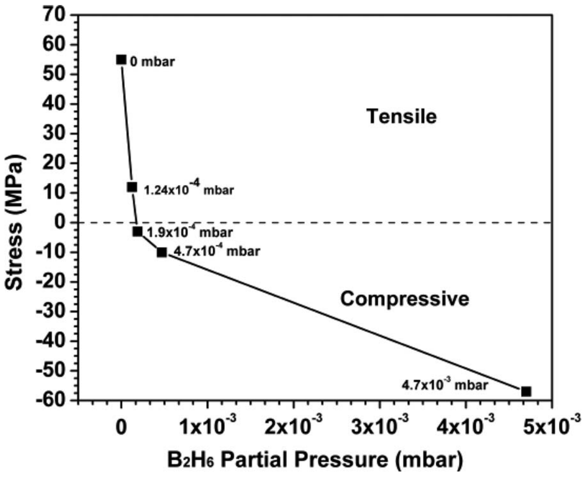

Figure 3. Stress in $Ge_{0.7}Si_{0.3}$ film versus diborane partial pressure, deduced from wafer bow.

Fig. 3 shows the stress determined from wafer curvature experiments. The measurement errors in stress are minimized by keeping the same number of data points for pre-deposition and post-deposition scans and using appropriate fixtures to ensure the scans overlap precisely. A deviation of 5% from the measured values of stress needs to be taken into account due to the possible error in the height data by stylus deflection. We observe a transition from tensile to compressive with increasing B_2H_6 partial pressure, around the point of lowest resistivity (cf. Fig. 2). A standard deviation of up to 11 MPa, within-batch, is found for the deposited layers. Therefore, the stress in $Ge_{0.7}Si_{0.3}$ layers can be tuned by the degree of incorporation of boron atoms.

Figure 4a shows the XRD spectra of deposited $Ge_{0.7}Si_{0.3}$ layers versus B_2H_6 partial pressure. The observed diffraction peaks from left to right correspond to the (111), (220) and (311) crystal planes of GeSi signifying the diamond like cubic crystal structure. The presence of these peaks in the XRD spectra can indicate the growth of V-shaped and columnar grains under the specified deposition conditions. The measured diffraction peaks are closer to pure-Ge peaks than to pure-Si; an average 73% Ge content is calculated for polycrystalline samples using Vegard's law.[16] The distinct diffraction peaks observed on layers deposited at low B_2H_6 partial pressure indicate polycrystalline material. The broadening of these peaks (Fig. 4a) indicates a decrease in grain size with an increase of B_2H_6 partial pressure. This is quantified by calculation of the average grain size with Scherrer's equation,[17] as presented in Fig. 4b. The grain size decreases from ∼30 nm to ∼5 nm as the B_2H_6 partial pressure increases from 0 mbar to $2.35 \cdot 10^{-3}$ mbar. The layers turn to amorphous with a B_2H_6 partial pressure above $4.7 \cdot 10^{-4}$ mbar, as evident from the XRD foot prints of Fig. 4a.

HR-SEM images of poly $Ge_{0.7}Si_{0.3}$ layers for $1.9 \cdot 10^{-4}$ mbar and $4.7 \cdot 10^{-4}$ mbar B_2H_6 partial pressures are shown in Fig. 5. The decrease in the grain size with increased B_2H_6 partial pressure can be observed from these images and is in line with the conclusion drawn from the XRD data.

The root-mean-square (RMS) surface roughness of 500-nm-thick layers deposited at a B_2H_6 pressure of $4.7 \cdot 10^{-4}$ mbar or higher is less than 0.7 nm. An RMS roughness up to 3.6 nm is measured on the polycrystalline samples.

Using XPS, the atomic concentrations of Ge and Si were determined to be 71% ± 2% and 29% ± 2%, respectively. The Ge fraction varies less than the measurement accuracy under the increase of B_2H_6 partial pressure from 0 mbar to $4.7 \cdot 10^{-3}$ mbar – see Fig. 6a. Fig. 6b shows the depth profile of a thick (∼1500 nm) poly $Ge_{0.7}Si_{0.3}$ layer deposited at B_2H_6 partial pressure of $4.7 \cdot 10^{-4}$ mbar. The Ge:Si ratio is constant across the entire layer.

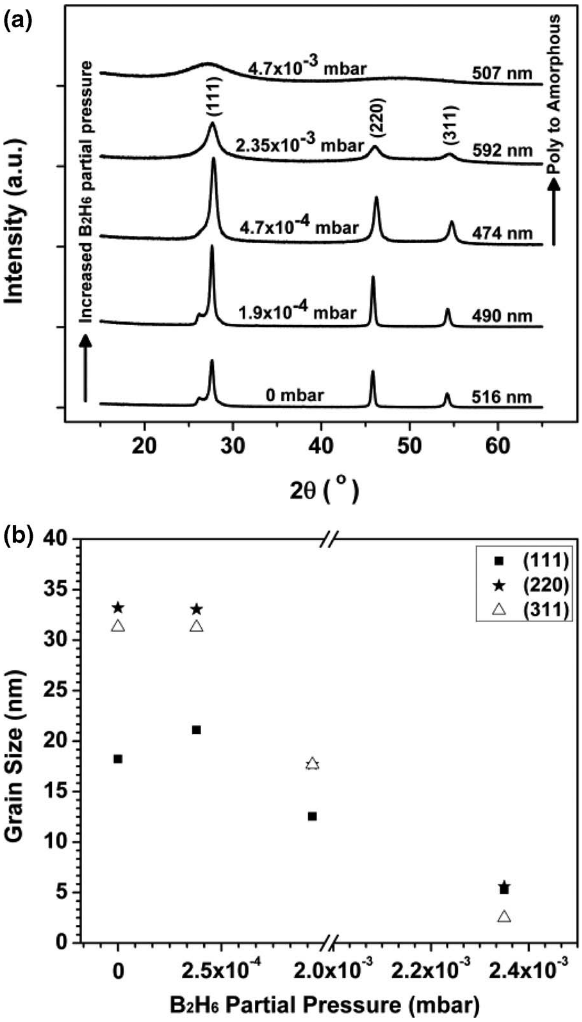

Figure 4. a) XRD footprints of LPCVD $Ge_{0.7}Si_{0.3}$ layers deposited with varying B_2H_6 partial pressures, showing the phase transition from polycrystalline to amorphous. (b) Grain size versus B_2H_6 partial pressure, calculated using Scherrer's equation[17] from the full width at half maximum (FWHM), extracted from XRD peaks after fitting with the Voigt method.[18]

SIMS analysis on samples with B_2H_6 partial pressure ranging from $1.24 \cdot 10^{-4}$ mbar to $4.7 \cdot 10^{-4}$ mbar confirms a uniform Ge to Si ratio. The atomic concentrations found are in good quantitative agreement with the XPS findings. The boron content is also examined with SIMS. At higher diborane partial pressure, a higher boron concentration is found in the films, with a more or less linear dependency in the studied process window: see Fig. 7. The boron is further found to be uniform throughout the $Ge_{0.7}Si_{0.3}$ layers (as visualized for one sample in the inset). The boron concentration is determined after calibration with a boron-doped silicon sample, which may lead to some systematic error.

A saturation limit for the *active* boron concentration of about $5.0 \cdot 10^{20}$ cm^{-3} was reported for poly GeSi layers deposited at 550°C.[19] We expect that the *active* boron concentration in our samples is even lower than the above value due to the lower deposition temperature (430°C). This may partly explain why the resistance does not further decrease above $1.9 \cdot 10^{-4}$ mbar (cf. Fig. 2) while the chemical boron concentration still rises. The change from polycrystalline via nanocrystalline to amorphous also reduces the conductivity of the samples produced with high diborane partial pressure.

Table I displays the key results of this work for 490 nm and 1500 nm thick $Ge_{0.7}Si_{0.3}$ films deposited at 430 °C, without annealing, together with the results reported in earlier publications treating in-situ doped polycrystalline GeSi films. The thinner films, deposited at the optimal diborane partial pressure of $1.9 \cdot 10^{-4}$ mbar, demonstrate

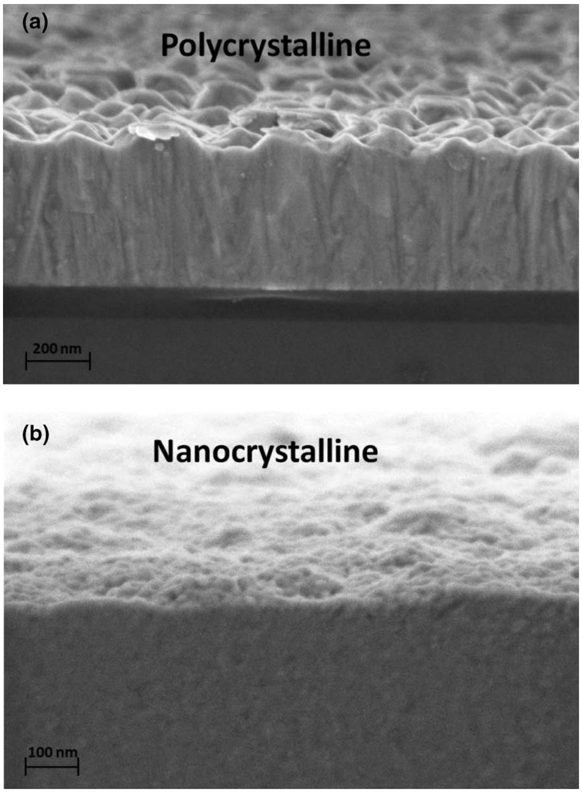

Figure 5. HR-SEM images of poly-$Ge_{0.7}Si_{0.3}$ layers deposited a) $1.9 \cdot 10^{-4}$ mbar; b) $4.7 \cdot 10^{-4}$ mbar of B_2H_6 partial pressures.

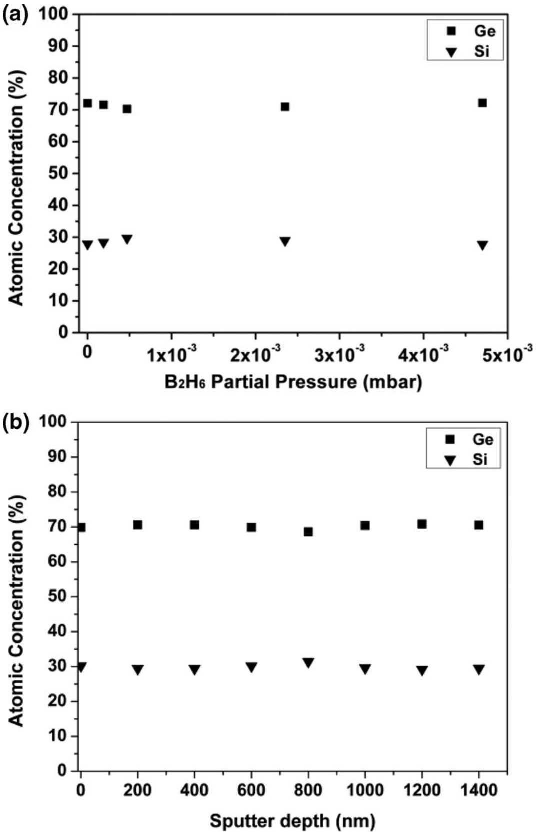

Figure 6. XPS depth profile on GeSi samples (a) Ge and Si contents with varying B_2H_6 partial pressures (b) ∼1500 nm poly $Ge_{0.7}Si_{0.3}$ film deposited at B_2H_6 partial pressure of $4.7 \cdot 10^{-4}$ mbar.

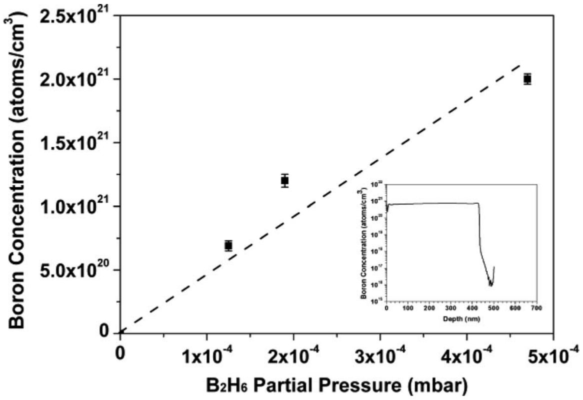

Figure 7. Boron concentration versus B_2H_6 partial pressure measured by SIMS. The dashed line represents the linear fit for the data points. The inset shows a continuous line indicating a uniform boron depth profile throughout the layer thickness deposited at B_2H_6 partial pressure of $1.24 \cdot 10^{-4}$ mbar.

better properties compared to the references in Table I, despite the relatively low deposition temperature. We attribute these improved values to the choice of B_2H_6,and the optimization of diborane partial pressure (Figs. 2 and 3).

For reasons of convenience, the thicker films directly implemented in GeSi-based RF microresonators (see the forthcoming section) are deposited at B_2H_6 partial pressure of $4.7 \cdot 10^{-4}$ mbar, which is slightly off the optimum pressure. The batch to batch uniformity in thickness and resistivity is found to be within 2% for these deposition conditions. These thicker layers exhibit the stress and resistivity of −29 MPa and 0.92 mΩ-cm, respectively.

It is important to note that, after exceeding certain films thickness, we expect no further increase in the stress due to the linear relationship between the bowing and the film thickness. Such a saturation of the stress value was observed for e.g. SiO_2 layers deposited by PECVD.[20] The deposition of few-μm thick layers (needed for certain MEMS applications) using LPCVD may be practically limited due to prolonged deposition time (several hours). In case of CMOS post-processing, this can affect the performance of underlying circuitry.

GeSi based RF Microresonators

The low stress and the low resistivity of the layers deposited at low B_2H_6 partial pressure allows application of in-situ boron doped GeSi as structural layers for suspended MEMS structures. Capacitively transduced micromechanical resonators (as reviewed in[24]) were fabricated using two stacked layers of in-situ doped $Ge_{0.7}Si_{0.3}$ with 1.5 μm thickness, separated by a thin sacrificial SiO_2 film. The suspended membranes remain in place and do not warp, bend or curl, as confirmed by SEM and microscope inspections on devices and test patterns. Typical resonators are displayed in Fig. 8.

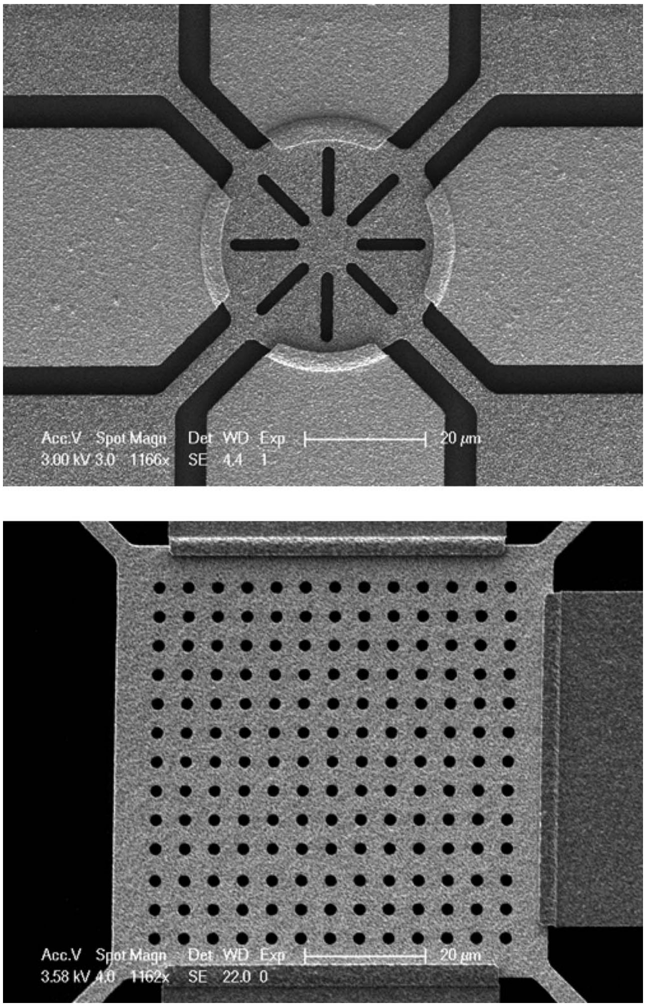

Figure 8. SEM images of the fabricated resonators with a maximum processing temperature of 430°C.

Fig. 9 shows the frequency response of the suspended MEMS resonator, excited in its Lamé mode exhibiting a resonance peak at 47.91 MHz with a motional impedance of 33 kΩ at a dc bias of 3 V over a transduction gap estimated to be 40 nm. The fabricated devices show quality factors well over 200,000 at atmospheric pressure,[25] the highest reported till date for post processing compatible capacitively transduced resonators.[26,27] The high quality factor achieved here, compared to commonly applied alternative thin-film materials, is possibly due to the reduced thermoelastic damping[28] and reduced surface losses[29] caused by the lattice defects and other imperfections

Table I. Key properties of the polycrystalline GeSi thin films of this work compared to earlier reported literature values. Of the 15 layers documented in,[13] the lowest-stress and lowest-resistivity results are listed here. We estimated the Ge fraction for this entry from the cited etch rate in H_2O_2 in line with Ref. 9. All films were deposited in LPCVD systems from SiH_4 and GeH_4.

Ref.	Film thickness (nm)	Stress (MPa)	Doping precursor	Resistivity (mΩ-cm)	Deposition temp. (°C)	Anneal temp. (°C)	Ge content (%)
9	Unspec.	Unspec.	PH_3	20	400	–	65%
21	2000	+300	PH_3	20	450	650	72%
13	1700	−53	BCl_3	19	440	–	∼75%
13	2600	−161	BCl_3	0.96	410		∼70%
22	Unspec.	+50	B_2H_6	1	400	520	69%
9	3100	−10	B_2H_6	1.8	450	–	65%
23	Unspec.	Unspec.	B_2H_6	0.66	525	–	73%
This Work	490	−3	B_2H_6	0.6	430	–	71%
This Work	1500	−29	B_2H_6	0.92	430	–	70%

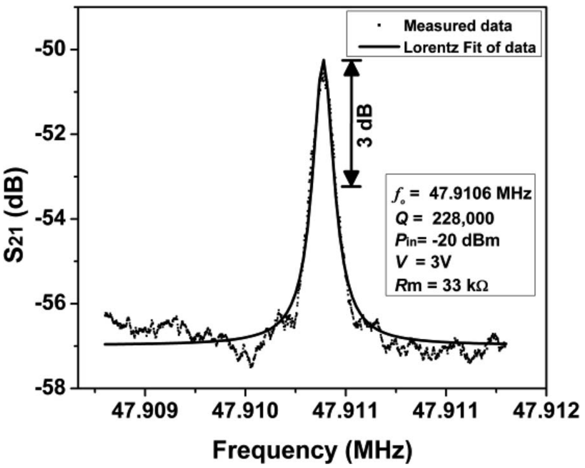

Figure 9. Measured frequency response of 40 μm by 40 μm square-plate resonator vibrating in Lamé mode.

that acts as a source of energy dissipation in micromechanical resonators.

Conclusions

We have deposited in-situ boron doped poly $Ge_{0.7}Si_{0.3}$ layers from SiH_4, GeH_4 and B_2H_6. We have studied the effects on resistivity, stress, texture, surface roughness and Ge/Si/Boron depth profile with varied B_2H_6 partial pressures, for fixed SiH_4 and GeH_4 partial pressures. The experiments show that the introduction of B_2H_6 hardly affects the Ge to Si ratio in the deposited layers. The stress in the layers varies from tensile to compressive, with lowest stress of 3 MPa compressive around $1.9 \cdot 10^{-4}$ mbar of B_2H_6 partial pressure; at the same partial pressure, a minimum in the resistivity of 0.6 mΩ-cm is measured. Amorphous material deposits at high B_2H_6 partial pressures, leading to high sheet resistance and reduced surface roughness. The fabrication of operational MEMS structures with a maximum process temperature of 430°C shows the potential of these layers as MEMS structural material for low-temperature microtechnologies such as CMOS-MEMS post-processing.

Acknowledgment

The authors thank M.A. Smithers and G.A.M. Kip from MESA$^+$ Institute of Nanotechnology for HR-SEM imaging and XPS characterization, respectively. The authors gratefully acknowledge M. A. Yaqoob (CTW, University of Twente) for RMS surface roughness analyzes, J. van Berkum and J. H. M. Snijders (both from MiPlaza, Philips Eindhoven) for their support for SIMS analyzes on the samples. We also thank our colleagues B. Rangarajan and J. Lu for their help with XRD measurements. This work is financially supported by the Dutch Technology Foundation STW through project grant no. 10048.

References

1. D. J. Paul, *Semicond. Sci. Technol.*, **19**, R75 (2004).
2. T. J. King, J. R. Pfiester, J. D. Shott, J. P. McVittie, and K. C. Saraswat, *Dig. – Int. Electron Devices Meet.*, 253–256, (1990).
3. C. Salm, D. T. van Veen, D. J. Gravesteijn, J. Holleman, and P. H. Woerlee, *J. Electrochem. Soc.*, **144**, 3665 (1997).
4. T. Ghani et al., *Dig. – Int. Electron Devices Meet.*, 978–980, (2003).
5. A. Kovalgin and J. Holleman, *J. Electrochem. Soc.*, **153**, G363 (2006).
6. H. Takeuchi, A. Wung, X. Sun, R. T. Howe, and T. J. King, *IEEE Trans. on Electron Devices*, **52**, 2081 (2005).
7. J. Schmitz, *Nucl. Instrum. Methods Phys. Res. Sect. A*, **576**, 142 (2007).
8. C. Leinenbach, H. Seidel, T. Fuchs, S. Kronmueller, and F. Laermer, *Proc. IEEE MEMS*, 65–68 (2007).
9. A. E. Franke, J. M. Heck, T. J. King, and R. T. Howe, *J. Microelectromech. Sys.*, **12**, 160 (2003).
10. A. Witvrouw et al., *ECS Trans.*, **33**(6), 799 (2010).
11. H. C. Lin, C. Y. Chang, W. H. Chen, W. C. Tsai, T. C. Chang, T. G. Jung, and H. Y. Lin, *J. Electrochem. Soc.*, **141**, 2559 (1994).
12. P. E. Hellberg, A. Gagnor, S. L. Zhang, and C. S. Petersson, *J. Electrochem. Soc.*, **144**, 3968 (1997).
13. C. W. Low, T. J. King Liu, and R. T. Howe, *J. Microelectromech. Sys.*, **16**, 68 (2007).
14. P. Peshev, *J. Solid State Chem.*, **154**, 157 (2000).
15. G. Stoney, *Proc. R. Soc. London A*, **82**, 172 (1909).
16. R. W. Cahn, *Physical Metallurgy*, North-Holland, Amsterdam (1965).
17. P. Scherrer, *Nachrichten Göttingen Gesellschaft*, **2**, 98 (1918).
18. R. A. Young and D. B. Wiles, *J. Appl. Cryst.*, **15**, 430 (1982).
19. A. Moriya, M. Sakuraba, T. Matsuura, and J. Murota, *Thin Solid Films*, **343–344**, 541 (1999).
20. V. Au, C. Charles, D. A. P. Bulla, J. D. Love, and R. W. Boswell, *J. Appl. Phys*, 084912 (2005).
21. Y. C. Jeon, T. J. King, and R. T. Howe, *J. Electrochem. Soc.*, **150**, H1 (2003).
22. S. Sedky, A. Witvrouw, and K. Baert, *Sensors and Actuators A: Physical*, **97–98**, 530 (2002).
23. V. Z-Q Li, M. R. Mirabedini, R. T. Kuehn, J. J. Wortman, and M. C. Öztürk et al., *Appl. Phys. Lett.*, **71**, 3388 (1997).
24. C. T. C. Nguyen, *IEEE Trans. Ultrasonics, Ferroelectrics and Frequency Control*, **54**(2), 251 (2007).
25. S. N. R. Kazmi, A. A. I. Aarnink, C. Salm, and J. Schmitz, *Proc. Int. Freq. Control Symp.*, Baltimore 2012.
26. W.-L. Huang, Z. Ren, and C. T.-C. Nguyen, *IEEE Int. Frequency Control Symp.*, 839–847 (2006).
27. H. Chandrahalim, S. A. Bhave, E. P. Quévy, and Roger T. Howe, *Proc. Transducers & Eurosensors*, 313–316 (2007).
28. C. Zener, *Phys. Rev.*, **53**(1), 90 (1938).
29. K. Y. Yasumura, T. D. Stowe, E. M. Chow, T. Pfafman, T. W. Kenny, B. Barry, C. Stipe, and D. Rugar, *Microelectromech. Syst.*, **9**(1), 117 (2000).